Influence of Docosahexaenoic Acid and Cholesterol on Lateral Lipid Organization in Phospholipid Mixtures[†]

Daniel Huster,[‡,§] Klaus Arnold,[§] and Klaus Gawrisch*[,‡]

Laboratory of Membrane Biochemistry and Biophysics, NIAAA, National Institutes of Health, 12420 Parklawn Drive, Room 158, Rockville, Maryland 20852, and Institute of Medical Physics and Biophysics, University of Leipzig, Liebigstrasse 27, 04103 Leipzig, Germany

Received January 12, 1998; Revised Manuscript Received August 25, 1998

ABSTRACT: We investigated lateral lipid organization in membranes with a lipid composition relevant to neural and retinal membranes [phosphatidylcholine (PC)/phosphatidylethanolamine (PE)/phosphatidylserine (PS)/cholesterol, 4/4/1/1, mol/mol/mol/mol]. The mixed-chain phospholipids contained saturated stearic acid (18:0) in the *sn*-1 position and the monounsaturated oleic acid (18:1) or polyunsaturated docosahexaenoic acid (22:6) in *sn*-2. Lateral lipid organization was evaluated by ^{2}H NMR order parameter measurements on stearic acid of all individual types of phospholipids in the mixture and, through a novel approach, two-dimensional NOESY ^{1}H NMR spectroscopy with magic angle spinning (MAS). The docosahexaenoic acid chain order was evaluated from ^{1}H NMR chain signal MAS-sideband intensities. Averaged over all lipids, the cholesterol-induced increase in *sn*-1 chain order is 2-fold larger in monounsaturated than in polyunsaturated lipids, and the order of both saturated and polyunsaturated hydrocarbon chains increases. Addition of cholesterol increases lipid order in the sequence 18:0-18:1 PE > 18:0-18:1 PC > 18:0-18:1 PS for the monounsaturated and 18:0-22:6 PC ≫ 18:0-22:6 PE > 18:0-22:6 PS for polyunsaturated mixtures. The variation of order parameters between lipid species suggests that cholesterol induces the formation of lipid microdomains with a headgroup and chain unsaturation-dependent lipid composition. The preferential interaction between cholesterol and polyunsaturated 18:0-22:6 PC, followed by 18:0-22:6 PE and 18:0-22:6 PS, was confirmed by ^{1}H MAS NOESY cross-relaxation rate differences. Furthermore, cholesterol preferentially associates with saturated chains in mixed-chain lipids reflected by higher saturated chain-to-cholesterol cross-relaxation rates. We propose that cholesterol forms PC-enriched microdomains in the polyunsaturated 18:0-22:6 PC/18:0-22:6 PE/18:0-22:6 PS/cholesterol membranes in which the saturated *sn*-1 chains are preferentially oriented toward the cholesterol molecules.

Not only are membrane bulk properties important for protein function, but local differences in these properties caused by an inhomogeneous lateral distribution of lipids in the bilayer are significant as well. Lipid domain formation may be triggered by differences in interaction energies between lipid species and between lipids and proteins. Extensive studies of binary lipid phase diagrams show that many lipids partially separate into crystalline domains when the temperature is lowered [see, e.g., (*1, 2*)]. Much less is known about the formation of fluid-phase lipid microdomains, enriched in specific lipid species, and imbedded in a fluid-phase matrix. It has been suggested that the tendency of proteins to interact with specific lipid domains is crucial for the assembly of membrane protein networks (*3*). Although the role of microdomains in cell membranes has been widely discussed (*3, 4*), there is little experimental evidence of their existence and their role in cell membrane function.

In this study, the lateral lipid organization in mixtures with a lipid composition relevant to neural membranes such as the retina was investigated. Neural membranes contain high levels of docosahexaenoic acid (22:6, DHA),[1] a long-chain, highly unsaturated ω3-fatty acid, which is essential for neural development and function (*5, 6*). From 20 to 50% of all fatty acids in the phospholipids of the retina are DHA (*7*). Inadequate concentrations of DHA in brain and retina have been related to impaired vision (*8*). Indeed, in experiments on model membranes it was established that both lipid headgroup composition and high concentrations of DHA in

[†] D.H. and K.A. acknowledge support by the Deutsche Forschungsgemeinschaft (SFB 197, A10) and D.H. support from the Studienstiftung des Deutschen Volkes.

* Corresponding author. Phone: (301) 594-3750. Fax: (301) 594-0035. E-mail: gawrisch@helix.nih.gov.

[‡] NIAAA, NIH.

[§] University of Leipzig.

[1] Abbreviations: NMR, nuclear magnetic resonance; FID, free induction decay; MAS, magic-angle spinning; NOE, nuclear Overhauser enhancement; NOESY, nuclear Overhauser enhancement spectroscopy; ESR, electron spin resonance; ROS, rod outer segment; PC, phosphatidylcholine; PE, phosphatidylethanolamine; PS, phosphatidylserine; DHA, docosahexaenoic acid; 18:0-18:1 PC, 1-stearoyl-2-oleoyl-*sn*-glycero-3-phosphocholine; 18:0-18:1 PE, 1-stearoyl-2-oleoyl-*sn*-glycero-3-phosphoethanolamine; 18:0-18:1 PS, 1-stearoyl-2-oleoyl-*sn*-glycero-3-phosphoserine; 18:0-22:6 PC, 1-stearoyl-2-docosahexaenoyl-*sn*-glycero-3-phosphocholine; 18:0-22:6 PE, 1-stearoyl-2-docosahexaenoyl-*sn*-glycero-3-phosphoethanolamine; 18:0-22:6 PS, 1-stearoyl-2-docosahexaenoyl-*sn*-glycero-3-phosphoserine; 22:6-22:6 PC, 1,2-didocosahexaenoyl-*sn*-glycero-3-phosphocholine; 14:0-14:0 PC, 1,2-dimyristoyl-*sn*-glycero-3-phosphocholine; the subscript d35 denotes a perdeuterated stearic acid chain.

10.1021/bi980078g CCC: $15.00
Published on Web 11/13/1998

lipid hydrocarbon chains are needed to result in native membrane-like light-induced activation of the photoreceptor rhodopsin (*9*−*12*).

The major phospholipids in vertebrate rod outer segment (ROS) disk membranes are PC, PE, and PS in approximate molar ratios of 4/4/1 (*7*). Furthermore, the membranes contain on average about 10 mol % cholesterol (*7*). ROS membranes vary in cholesterol to phospholipid molar ratio from 0.30 to 0.05, with the higher cholesterol content in the basal, newly synthesized disks, and the lower cholesterol content at the apical tip (*13, 14*). A large number of studies on cholesterol−phospholipid interaction have been conducted, but only a few general features of that interaction were established.

Binary mixtures of cholesterol and saturated PCs have a complex phase diagram. The existence of cholesterol-enriched (liquid-ordered) and cholesterol-depleted (liquid-disordered) phases was observed (*15*−*18*). Van Dijck et al. (*19*) reported a preference of cholesterol for interaction with PC in ternary PC/PE/cholesterol mixtures. Studies on the distribution of cholesterol between vesicles of different lipid composition indicated a preference of cholesterol for interaction with PC (*20*). However, investigations by Blume (*21*) and Tilcock et al. (*22*) showed no preferential affinity of cholesterol for either PC or PE. Van Dijck investigated cholesterol's affinity for negatively charged phospholipids, like PS, in ternary PS/PE-or-PC/cholesterol mixtures by calorimetry, and concluded that the negatively charged lipid has a higher affinity to cholesterol (*23*). In contrast, experiments by Bach et al. (*24*) suggest a reduced affinity of cholesterol to PS.

Recent investigations indicated that the nature of cholesterol−phospholipid interactions, and thus the miscibility of cholesterol in the bilayer, depends on both the structure of the phospholipid polar headgroup and the hydrocarbon chains (*25*). An influence of chain length as well as of chain unsaturation on cholesterol−phospholipid interaction was reported. In binary mixtures of short- and long-chain saturated PCs, addition of 50 mol % cholesterol abolished the lateral segregation of the PCs in the phase transition region, while lower cholesterol concentrations enhanced segregation (*26*). The stronger self-association of cholesterol in membranes of phospholipids with monounsaturated hydrocarbon chains, seen in ESR (*27, 28*), and the results of cholesterol transfer between liposomal membranes (*29, 30*) suggest less favorable interactions between cholesterol and unsaturated chains. Monolayer studies on binary PC/cholesterol mixtures using PCs with variable degrees of unsaturation demonstrated that PCs with two polyunsaturated hydrocarbon chains do not show cholesterol-induced area condensation (*31, 32*). In bilayer studies, it was detected that cholesterol does not remove the gel−liquid-crystalline phase transition of these lipids (*33*) suggesting that cholesterol does not interfere with the packing of di-polyunsaturated PCs.

There is less agreement regarding the influence of polyunsaturation in mixed-chain PCs with a saturated 16:0 or 18:0 chain in *sn*-1, and unsaturated chains in *sn*-2, on cholesterol−PC interaction. Demel (*34*) reported larger cholesterol-induced area condensation in mixed-chain PC with a monounsaturated *sn*-2 chain than in PCs with polyunsaturated chains. More recent monolayer studies by Smaby et al. (*31*), which were conducted at membrane-like surface pressures, observed no measurable difference in cholesterol-induced area condensation. However, the binary mixtures showed a remarkable difference of in-plane monolayer elasticity as a function of *sn*-2 chain unsaturation. At cholesterol mole fractions higher than 30 mol %, the PC species with higher *sn*-2 unsaturation levels show a smaller reduction of the in-plane monolayer elasticity with increasing unsaturation (*31*). Keough and colleagues (*35*−*37*) observed increased susceptibility of phase transition parameters of mixed-chain PCs to cholesterol as the number of double bonds in the *sn*-2 chains increased from zero to two, and decreased susceptibility for *sn*-2 chains with four (20:4) and six (22:6) double bonds. Preliminary results of monolayer pressure−area isotherm investigations on 18:0-18:1 PC/18:0-22:6 PC/cholesterol mixtures also suggested that cholesterol interacts more strongly with the monounsaturated PC (*38*).

The investigation of lateral lipid organization in biological membranes is a formidable challenge. Calorimetry reports lipid mixing behavior in the phase transition region. It remains to be demonstrated that these data apply also to the biologically relevant liquid-crystalline phase. Also, the applicability of monolayer investigation to bilayer studies is debated. There is a strong need for new methods, capable of studying clusters and domains with dimensions in the submicrometer range, that can be applied to protein-containing lipid bilayers and do not require incorporation of perturbing labels.

In this study, two NMR methods were used to investigate lateral lipid organization. First, we measured ^{2}H NMR chain order parameters of all individual phospholipids in 1-stearoyl$_{d35}$-2-oleoyl-PC/PE/PS (4/4/1, mol/mol/mol) and 1-stearoyl$_{d35}$-2-docosahexaenoyl-PC/PE/PS (4/4/1) mixtures with and without 10 mol % cholesterol. The lipid hydrocarbon chains in pure PC, PE, and PS membranes have somewhat different order parameters (*39*−*42*). It is expected that these differences vanish in ideal mixtures of lipids with different headgroups but identical hydrocarbon chains. Addition of cholesterol to the mixture results in phospholipid area condensation, reflected as a drastic increase in chain order (*43, 44*). Partial separation of lipids into domains is detected via differences in chain order parameters between the lipids, even when they exchange rapidly between domains.

In a second series of experiments, we measured the rate of magnetization transfer between proton resonances of the different lipid species and cholesterol in quaternary lipid mixtures by nuclear Overhauser enhancement spectroscopy. The idea for this approach came from earlier measurements by Yeagle et al. (*45, 46*) that demonstrated the use of magnetization transfer between lipid molecules for bilayer studies. Recent developments in high-resolution MAS technology (*47, 48*) enabled us to determine cross-relaxation rates in a more direct fashion by using a two-dimensional NOESY approach. Principles of quantitative data analysis have been tested in experiments on 14:0-14:0 PC (Huster et al., submitted for publication). Here, we demonstrate that the rates of magnetization transfer between lipid species contain valuable information about segregation of lipids into microdomains. The NOESY experiments not only reflected the preference of cholesterol for interaction with the polyun-

saturated 18:0-22:6 PC in PC/PE/PS/cholesterol mixtures, but also discriminated between interaction of cholesterol to the saturated (18:0) and the polyunsaturated (22:6) chain in mixed-chain 18:0-22:6 PC.

MATERIALS AND METHODS

Materials. The phospholipids and cholesterol were purchased from Avanti Polar Lipids Inc. (Alabaster, AL). Lipid purity was checked by HPLC before and after the experiments and judged to be near 98%. The phospholipids containing DHA were stored in organic solvent at −60 °C with butylated hydroxytoluene (BHT) added at a lipid/BHT ratio of 250/1 to prevent DHA oxidation. Cholesterol$_{d7}$ (25,26,26,26,27,27,27-*d*7, 98%) was purchased from Cambridge Isotope Laboratories (Andover, MA).

Sample Preparation. DHA-lipid sample preparation was carried out in a Plexiglas glovebox under an argon atmosphere. Known quantities of each lipid dissolved in organic solvent were mixed in a glass tube, and the solvent was removed under a stream of argon. The lipid films were redissolved in about 500 μL of cyclohexane (depleted in oxygen by aeration with argon), and the solution was frozen in liquid nitrogen. Samples were freeze-dried at a pressure of 50 μmHg for 4 h, resulting in a fluffy lipid powder which is easier to handle in consecutive preparation steps. Small aliquots of lipid (1 wt %) were dispersed in a buffer solution containing 100 mM NaCl, 10 mM HEPES buffer, adjusted to pH 7.4. Either D_2O, for ^{1}H NMR experiments, or deuterium-depleted water, for ^{2}H NMR experiments, was used to prepare the buffer solution. Samples were equilibrated in 10 freeze−thaw cycles. Suspensions were transferred to Eppendorf centrifuge containers and centrifuged at 27000*g* for 5 min. For ^{2}H and ^{31}P NMR experiments, lipid pellets were transferred to 5 mm glass sample tubes equipped with a ground glass joint and cap. The ground glass joint was coated by a thin film of Teflon grease to prevent oxygen from entering the sample and the cap further secured with a layer of Parafilm. For MAS NMR experiments, suspensions were ultracentrifuged at 100000*g* for 2 h, and the lipid pellet was transferred to a home-built Kel-F insert for 4 mm MAS rotors which accommodates a sample volume of approximately 8 μL.

^{2}H and ^{31}P NMR. The ^{2}H NMR spectra were acquired on a Bruker DMX300 spectrometer (Billerica, MA) at a frequency of 46.06 MHz and a spectral width of 200 kHz using a high-power probe with a 5 mm solenoid coil. A phase-cycled quadrupolar echo pulse sequence was used (*49*) with 2.1 μs 90° pulses, a 50 μs delay between pulses, and a relaxation delay of 0.5 s. The carrier frequency of the instrument was placed at the center of the spectrum. Typically 50 000−500 000 scans were accumulated in the quadrature detection mode. The free induction decays were phased to zero the signal in the imaginary channel. Then, the time of the echo maximum in the real signal channel was determined with a resolution of one-tenth of a dwell time unit by fitting a spline function to the data points. Spline interpolation was also used to calculate free induction decay signals in real and imaginary channels that are time base corrected to start exactly at the echo maximum. An exponential line broadening of 100 Hz was applied to the free induction decay before Fourier transformation. Because of spectral symmetry, the signal in the imaginary channel contains only noise and was usually discarded for dePaking to gain in signal-to-noise by the factor of 1.41. DePaked spectra (*50*) were calculated using the algorithm of McCabe and Wassall (*51*). To derive the order parameter profile for each carbon along the deuterated chain, we integrated dePaked spectra over the peak areas that were due to methylenes in the *sn*-1 chain (*52*). It was assumed that each methylene group contributes equal intensity to the dePaked spectrum and that order increases in a smooth fashion from the terminal methyl group to the carbonyl group. The integral was divided into 32 steps and then averaged over 2 steps to yield 16 quadrupole splittings corresponding to each of the methylene segments in the stearic acid chain. The terminal methyl splitting can be assigned unambiguously and was obtained directly from the dePaked spectrum. Order parameters were calculated assuming a quadrupole coupling constant $e^2qQ/h = 167$ kHz. For the calculation of the average order parameter, a "final" methylene order parameter S_{18} was extrapolated from a linear fit of the last two points ($S_{16}-S_{17}$) of the step function (*52*). Average order parameters were calculated by adding all order parameters and dividing them by the number of deuterated groups in the chain. We compared average order parameters between symmetrized and nonsymmetrized spectra and found agreement within the experimental error margin of $\Delta S = \pm 0.002$. All data processing starting from the manipulation of the free induction decay was done with a program written for Mathcad (Mathsoft, Inc., Cambridge, MA).

^{31}P NMR spectra were accumulated at a resonance frequency of 121.47 MHz and a spectral width of 125 kHz using a Hahn-echo, 90°−τ−180°−τ−acquire, pulse sequence with a delay time, τ, of 39 μs, a 90° pulse length of 1.6 μs, and a relaxation delay of 1 s. Broadband proton decoupling was used during the pulse and acquisition periods. A 20 Hz line broadening was applied to the FID before Fourier transformation.

Unless stated otherwise, all measurements were carried out at a temperature of 25 °C.

MAS NMR. Magic angle spinning NMR experiments were carried out on a Bruker DMX500 spectrometer (Billerica, MA). Samples were spun at 5 kHz using a Bruker double gas bearing MAS probehead for 4 mm rotors operating with nitrogen gas. ^{1}H NMR experiments were carried out at a resonance frequency of 500.13 MHz using a spectral width of 3.3 kHz and a 90° pulse length of 4.5 μs.

Proton spinning sideband intensities as a function of spinning speed were recorded in MAS spectra accumulated at a spectral width of 40 kHz. Spinning speeds were varied between 1800 and 5000 Hz and controlled with a precision of ±1 Hz by the Bruker pneumatic MAS control unit. Sideband intensities were normalized by dividing them by centerband intensities.

Two-dimensional MAS nuclear Overhauser enhancement spectroscopy (NOESY) experiments (*53*, *54*) were carried out in a phase-sensitive mode. For representative samples, NOE build-up curves were recorded as a function of mixing times ranging from 5 to 1000 ms. In all other experiments, mixing times of 150 and 300 ms were chosen for optimal cross-peak intensity with acceptably low perturbation from relaxation effects. A total of 512 t_1 increments with 8, 16, or 24 scans per increment and a relaxation delay of 4 s

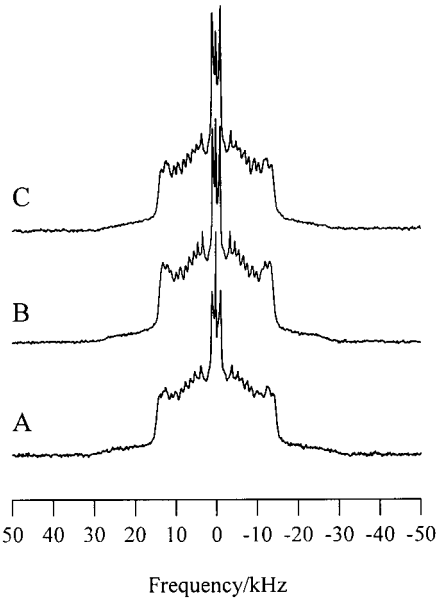

FIGURE 1: ^{2}H NMR powder spectra of 18:0$_{d35}$-22:6 PS (A), 18:0$_{d35}$-22:6 PE (B), and 18:0$_{d35}$-22:6 PC (C) in a 18:0-22:6 PC/PE/PS (4/4/1, mol/mol/mol) mixture. Small differences in chain order parameters of the individual lipids in the mixture have been detected.

between scans were acquired, yielding total acquisition times of 5−15 h per spectrum. The magnetic field strength was locked using the D_2O resonance signal from the spinning sample.

Cross-peak volumes in NOESY spectra were calculated with AURELIA software (Bruker Instruments, Inc., Billerica, MA) by a process of iterative segmentation. The segmentation starts at the top of each peak and advances down recursively until data points of other peaks or the base line level are reached. In spectra recorded at one mixing time, cross-relaxation rates were calculated by the formula $\sigma_{BA} = I_{AB}/I_A\tau$, where I_{AB} is the cross-peak volume, I_A the lipid diagonal peak volume from which migration of magnetization starts, and τ the mixing time. In selected cases, cross-peak volume was recorded as a function of mixing time, and NOE build-up curves were fitted to a spin-pair interaction model (*55*, *56*) using the nonlinear regression curve fitter in SigmaPlot (Jandel Scientific Software, San Rafael, CA).

RESULTS

According to the anisotropy of chemical shift of phospholipid ^{31}P NMR powder spectra, all investigated phospholipid and phospholipid−cholesterol mixtures were in a lamellar liquid-crystalline phase (data not shown). A typical series of ^{2}H NMR powder spectra of *sn*-1 chain perdeuterated stearic acid in 18:0-22:6 PC/18:0-22:6 PE/18:0 -22:6 PS mixtures (4/4/1) is presented in Figure 1. By labeling the stearic acid chain of either PC, PE, or PS in the mixture, the order parameters of all three phospholipids in the mixed membranes could be individually studied. Smoothed chain order parameter profiles (Figure 2) were calculated from the ^{2}H NMR powder patterns using the procedure described under Materials and Methods. For comparison of order between lipid species, average order parameters of the entire stearic acid chain were determined (Tables 1 and 2).

Chain Order in Single Phospholipid Membranes and PC/PE/PS Mixtures. The chain order at 25 °C of pure 18:0-18:1 PC, 18:0-18:1 PE, and 18:0-18:1 PS can be compared with the chain order of the same lipids in 18:0-18:1 PC/18:0-18:1 PE/18:0-18:1 PS (4/4/1, mol/mol/mol) mixtures. Order parameters of pure 18:0-18:1 PE have been determined at a slightly higher temperature (35 °C) because this lipid has its main phase transition at 30 °C, and converts to a

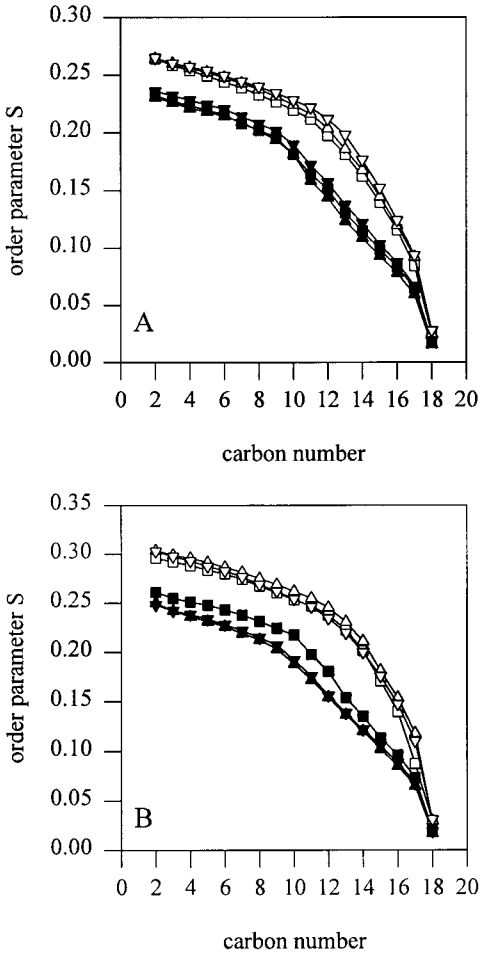

FIGURE 2: Stearic acid (18:0$_{d35}$) ^{2}H NMR order parameter profiles in monounsaturated 18:0-18:1 PC/PE/PS (4/4/1, mol/mol/mol) (open symbols) and polyunsaturated 18:0-22:6 PC/PE/PS/ (4/4/1/1) (filled symbols) mixtures. Panel A depicts the order parameter profiles without addition of cholesterol, and panel B the profiles after addition of 10 mol % cholesterol. In the polyunsaturated mixture, the order parameters of 18:0-22:6 PC increase much more than the order parameters of PE and PS, suggesting a preferential interaction between the polyunsaturated PC and cholesterol. PC (□, ■), PE (△, ▲), PS (▽, ▼).

Table 1: Average Order Parameters[a] at 25 °C of the Perdeuterated Stearic Acid Chain in Monounsaturated (18:0-18:1) and Polyunsaturated (18:0-22:6) Lipids[b]

	S_{av}	
lipid	18:0-18:1	18:0-22:6
PC_{d35}	0.158	0.149
PC_{d35}/PE/PS	0.196	0.162
PE_{d35}	0.217[c]	—[d]
PC/PE_{d35}/PS	0.201	0.159
PS_{d35}	0.189	0.164
PC/PE/PS_{d35}	0.204	0.169

[a] The experimental error is ±0.002. [b] Values for single lipids and for the same lipids in PC/PE/PS (4/4/1, mol/mol/mol) mixtures are given. [c] At 35 °C. [d] Pure 18:0-22:6 PE_{d35} converts to an inverse hexagonal phase at the main phase transition.

Table 2: Average Order Parameters[a] of Perdeuterated Stearic Acid in Monounsaturated (18:0-18:1) and Polyunsaturated (18:0-22:6) PC/PE/PS (4/4/1, mol/mol/mol) and PC/PE/PS/Cholesterol Mixtures (4/4/1/1, mol/mol/mol/mol)

	S_{av}		
cholesterol	0 mol %	10 mol %	ΔS_{av}
18:0-18:1			
PC_{d35}/PE/PS	0.196	0.226	+0.030
PC/PE_{d35}/PS	0.201	0.238	+0.037
PC/PE/PS_{d35}	0.204	0.231	+0.027
18:0-22:6			
PC_{d35}/PE/PS	0.162	0.186	+0.024
PC/PE_{d35}/PS	0.159	0.175	+0.016
PC/PE/PS_{d35}	0.169	0.178	+0.009

[a] The experimental error is ±0.002.

hexagonal phase at 70 °C. Pure 18:0-18:1 PE has the highest order followed by 18:0-18:1 PS and 18:0-18:1 PC. In the monounsaturated 18:0-18:1 PC/18:0-18:1 PE/18:0-18:1 PS mixture, slightly higher order was found for 18:0-18:1 PS followed by 18:0-18:1 PE and 18:0-18:1 PC. The 18:0-18:1 PE increases the order of both 18:0-18:1 PC and 18:0-18:1 PS, but the increase for 18:0-18:1 PC is larger, resulting in similar order parameter values for all three lipids.

The chain order of polyunsaturated DHA-containing phospholipids is lower [see also (*57*)], and differences in lipid order between lipid species are smaller. However, the sequence of relative differences in lipid order between pure lipid species is similar to the monounsaturated lipids: pure 18:0-22:6 PS has higher order than 18:0-22:6 PC. No data are available for pure 18:0-22:6 PE because it has a main phase transition at approximately 10 °C, and directly converts from the gel phase to the inverted hexagonal phase. Small order differences occur between lipid species in the polyunsaturated 18:0-22:6 PC/18:0-22:6 PE/18:0-22:6 PS (4/4/1, mol/mol/mol) mixtures, with higher order in 18:0-22:6 PS and somewhat lower order in 18:0-22:6 PC and 18:0-22:6 PE (see Table 1). The addition of 11 mol % 18:0-22:6 PS did not influence the lipid chain order of 18:0-22:6 PC and 18:0-22:6 PE compared to an equimolar 18:0-22:6 PC/18:0-22:6 PE mixtures. Average order parameters of 18:0-22:6 PC and 18:0-22:6 PE in this 1/1, mol/mol mixture are 0.163 and 0.159, respectively (J. A. Barry and K. Gawrisch, unpublished result).

Cholesterol-Induced Area Condensation. Area condensation was evaluated by measuring the cholesterol-induced increase in chain order. In Figure 2, order parameter profiles for mono- and polyunsaturated mixtures in the presence and absence of 10 mol % cholesterol are plotted. The average order parameters are given in Table 2. All polyunsaturated phospholipids show less area condensation due to cholesterol than the monounsatured phospholipids. The response of individual lipid species to cholesterol is also varied. In monounsaturated mixtures, a somewhat larger condensation is seen for 18:0-18:1 PE, followed by 18:0-18:1 PC and 18:0-18:1 PS. In the polyunsaturated mixture, cholesterol-induced lipid condensation is particularly sensitive to the phospholipid headgroup: 18:0-22:6 PC condenses the most followed by 18:0-22:6 PE and 18:0-22:6 PS. In both mono- and polyunsaturated mixtures, the PS has the highest order without cholesterol and the smallest cholesterol-induced area condensation.

Table 3: Cross-Relaxation Rates, $\sigma_{lipid-chol}$, between the Saturated *sn*-1 Chain Methylene Groups (1.30 ppm) of 18:0-22:6 PC, 18:0-22:6 PE, and 18:0-22:6 PS and the Cholesterol C_{18} Methyl Resonance (0.71 ppm) in 18:0-22:6 PC/PE/PS/Cholesterol Mixtures (4/4/1/3 mol/mol/mol/mol)[a]

lipid[b]	$\sigma_{lipid-chol}$ (s^{-1})	ΔS_{av}
PC	−0.057	+0.040
PE	−0.052	+0.030
PS	−0.040	+0.026

[a] For comparison, the cholesterol-induced increase in the *sn*-1 chain order, ΔS_{av}, in the same mixture is reported. [b] Contained a protonated stearic acid in the *sn*-1 position while the other two phospholipids were perdeuterated.

Cholesterol Interaction with 18:0-22:6 PC/18:0-22:6 PE/18:0-22:6 PS. To monitor *sn*-1 chain/cholesterol interaction, the intensity of the cross-peak between the chain methylene groups (1.3 ppm) of the lipid and the methyl group at carbon position C_{18} of cholesterol (0.71 ppm) in two-dimensional NOESY spectra was analyzed. $Cholesterol_{d7}$ was used to eliminate the overlap of the *sn*-1 chain methyl signal with the protons on cholesterol's carbon positions $C_{26,27}$. Again, selectivity of interaction to a particular lipid species was achieved by using protonated stearic acid in one of the lipid species in the 18:0-22:6 PC/18:0-22:6 PE/18:0-22:6 PS/$cholesterol_{d7}$ (4/4/1/3) mixture, and deuterated stearic acid in the other two. Absolute values of magnetization transfer between lipids are concentration dependent, and transfer rates to protons of the only 10 mol % cholesterol in the mixture have larger experimental errors. To improve precision, the NOESY experiments have been conducted at a cholesterol concentration of 25 mol %. Cross-relaxation rates for interactions between PC, PE, or PS and cholesterol are given in Table 3. The increase in average *sn*-1 chain order due to 25 mol % cholesterol as measured by ^2H NMR is listed in the last column of Table 3 for comparison. The highest cross-relaxation rate is observed for the interaction of 18:0-22:6 PC with cholesterol, followed by 18:0-22:6 PE and 18:0-22:6 PS. This is in good agreement with chain order parameter increases seen by ^2H NMR in these lipids. Cross-relaxation rates obtained in a NOESY experiment on a 18:0-22:6 PC/18:0-22:6 PE/cholesterol (1/1/0.67, mol/mol/mol) mixture confirmed the preferential interaction between cholesterol and 18:0-22:6 PC.

Cholesterol-to-Saturated versus Polyunsaturated Chain Interactions. These experiments were conducted on the saturated 14:0-14:0 PC, the polyunsaturated mixed-chain 18:0-22:6 PC, and the di-polyusatureated 22:6-22:6 PC at cholesterol concentrations from 0 to 50 mol %. Saturated 14:0-14:0 PC was chosen to be able to conduct the experiments at 25 °C. ^1H MAS NMR sideband intensities were recorded as a function of spinning speed to evaluate cholesterol-induced chain ordering. The nonspinning ^1H NMR spectrum of a 18:0-22:6 PC/cholesterol dispersion is shown in Figure 3A. Without MAS, the proton spectrum is broadened by strong dipolar interactions between protons. Only the signals of the mobile water molecules (HDO at 4.7 ppm), the γ-choline signal [$N(CH_3)_3$ at 3.25 ppm], and the terminal methyl groups (at 0.885 and 0.95 ppm) are partially resolved. With MAS, most of the signal intensity is collected into the narrow center band and a small fraction in the sidebands on both sides (*47*, *48*, *58*, *59*), the intensity

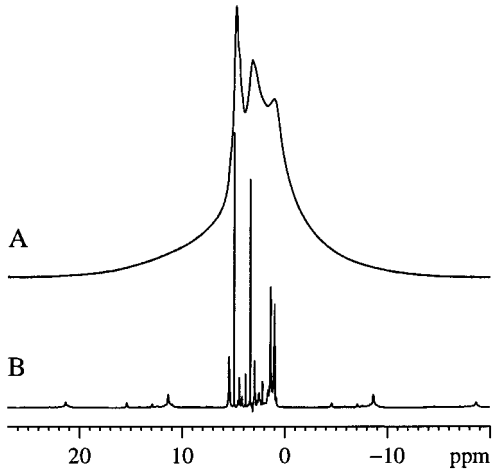

FIGURE 3: ^{1}H NMR spectra of a 18:0-22:6 PC/cholesterol mixture (1/1) dispersed in 50 wt % D_2O. (A) Static and (B) MAS spectrum at 5 kHz spinning speed. First- and second-order spinning sidebands are seen on both sides of the centerband at multiples of the spinning speed (5 kHz = 10 ppm).

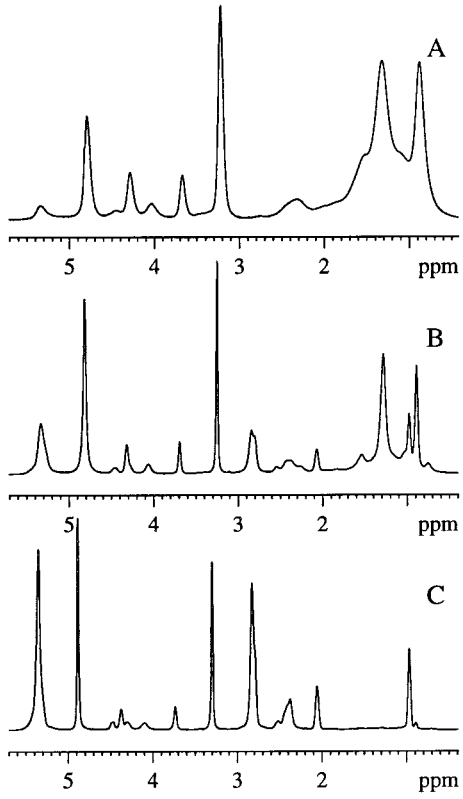

FIGURE 4: ^{1}H MAS spectra of 14:0-14:0 PC, 18:0-22:6 PC, and 22:6-22:6 PC mixtures with 50 mol % cholesterol. Strong interactions between the phospholipid and cholesterol broaden the 14:0-14:0 PC chain and glycerol resonances (A). In contrast, a 18:0-22:6 PC/cholesterol mixture showed well-resolved resonances of lipid and cholesterol (B). The 22:6-22:6 PC/cholesterol spectrum (C) has well-resolved lipid resonances, but most cholesterol signals are broadened beyond the detection limit, indicating that cholesterol forms crystallites and does not mix with di-polyunsaturated PC.

of which depends on the strength of ^{1}H−^{1}H dipole−dipole interaction and on spinning speed (*60, 61*).

The ^{1}H NMR MAS centerband spectra of 14:0-14:0 PC, 18:0-22:6 PC, and 22:6-22:6 PC mixed with 50 mol % cholesterol are shown in Figure 4. The 14:0-14:0 PC chain resonances became very broad after addition of cholesterol

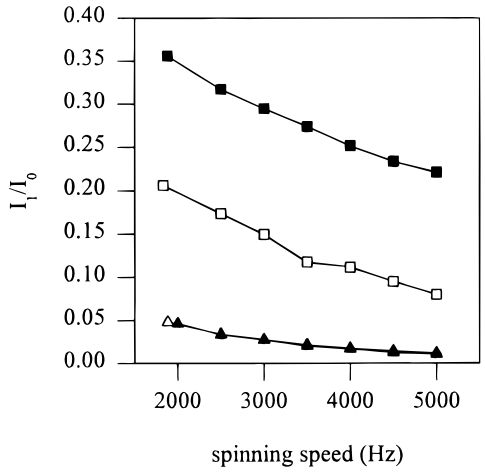

FIGURE 5: Normalized first-order MAS sideband intensities of 14:0-14:0 PC (□) and 22:6-22:6 PC (△) methylene chain signals. Addition of 50 mol % cholesterol increased the chain order of 14:0-14:0 PC (■) but has no influence on the order of 22:6-22:6 PC (▲).

(spectrum A), indicating strong immobilization of the lipid. For the mixed-chain, polyunsaturated 18:0-22:6 PC/cholesterol (spectrum B) and di-polyunsaturaed 22:6-22:6 PC/cholesterol mixtures (spectrum C), the lipid resonances remain well resolved after cholesterol addition. The cholesterol methyl group resonances C_{18} (0.71 ppm) and $C_{26,27}$ (0.885 ppm, overlapping with the *sn*-1 chain methyl group) are only seen in the 18:0-22:6 PC/cholesterol mixtures. In the 22:6-22:6 PC/cholesterol mixtures, most of the cholesterol signals are broadened beyond detection, suggesting that cholesterol forms a separate crystalline phase.

The normalized sideband intensities of the methylene groups of 14:0-14:0 PC and 22:6-22:6 PC in the presence (open symbols) and absence (filled symbols) of 50 mol % cholesterol are given in Figure 5. Sideband intensities of the saturated chains increase by almost 50% after cholesterol addition, corresponding to a large increase in lipid chain order. Normalized sideband intensities of the di-polyunsaturated 22:6-22:6 PC chain are much lower than 14:0-14:0 PC chain sidebands, indicating lower order parameters of the polyunsaturated chain. Furthermore, no increase in sideband intensity of the polyunsaturated chain is seen in the presence of 50 mol % cholesterol, supporting the hypothesis that 22:6-22:6 PC with two polyunsaturated chains and cholesterol do not mix.

Figure 6 depicts sideband intensities of 18:0 and 22:6 chains in mixed-chain18:0-22:6 PC. Again, sideband intensities of the saturated chain are higher than sideband intensities of the polyunsaturated chain. After cholesterol addition, *both* saturated *sn*-1 and polyunsaturated *sn*-2 chains *gained* in order. However, sideband intensities remained much lower than for the saturated 14:0-14:0 PC/cholesterol mixture. Lower sideband intensities are equivalent to lower chain order parameters.

Saturated versus polyunsaturated chain-to-cholesterol interactions in 18:0-22:6 PC were studied by an analysis of NOESY cross-relaxation rates. To increase precision in the calculated rates, experiments were conducted as a function of mixing time and analyzed according to the proton pair interaction model as outlined under Materials and Methods. In Figure 7A, a typical ^{1}H NOESY contour plot is shown

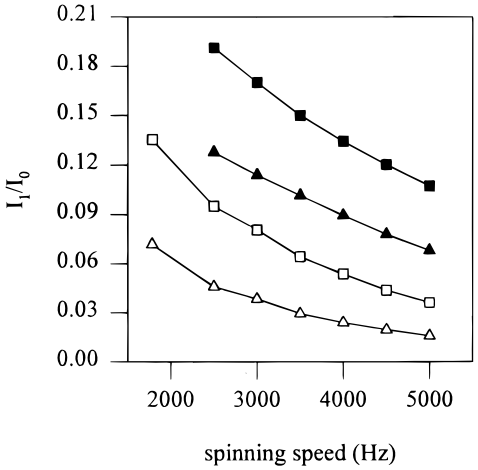

FIGURE 6: Normalized first-order MAS sideband intensities of saturated (18:0, □) and polyunsaturated (22:6, △) methylene chain signals in 18:0-22:6 PC. Addition of 50 mol % cholesterol increases the order of both chains (filled symbols).

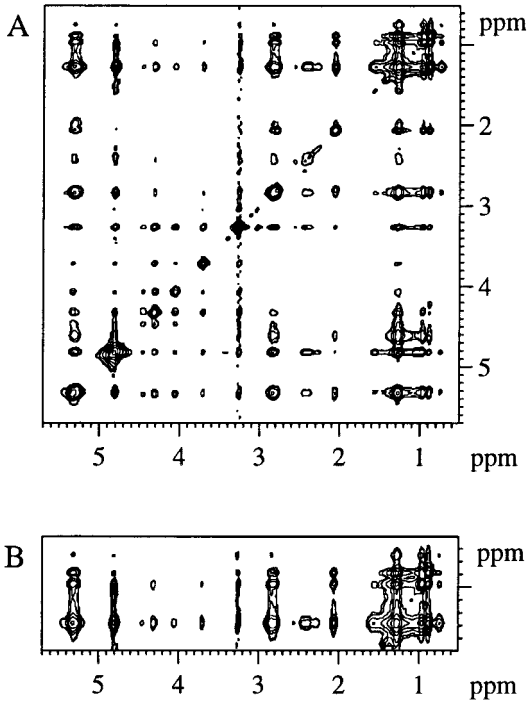

FIGURE 7: ^{1}H MAS NOESY contour plot of a 18:0-22:6 PC/cholesterol$_{d7}$ (1/1) mixture recorded at a mixing time of 300 ms (panel A). Panel B shows the lipid chain-to-cholesterol cross-peak region enlarged.

for a 18:0-22:6 PC/cholesterol$_{d7}$ mixture (1/1). Panel B shows the region of lipid−cholesterol cross-peaks. The intensity of the cross-peak between chain methylene and cholesterol C_{18} resonances, and of the corresponding diagonal peaks, as a function of mixing time is presented in Figure 8. The rates of magnetization transfer from saturated chain resonances to cholesterol are higher than the corresponding rates from polyunsaturated chain resonances to cholesterol, suggesting that cholesterol prefers contacts to saturated chains.

Cross-relaxation rates between 18:0-22:6 PC chain signals and cholesterol as a function of cholesterol concentration calculated from measurements at one mixing time are shown in Figure 9. This is an approximate approach to calculate

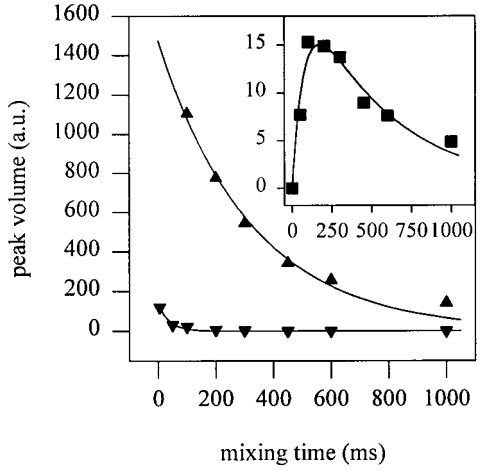

FIGURE 8: Intensity of diagonal- and cross-peaks as a function of mixing time in a 18:0-22:6 PC/cholesterol$_{d7}$ (1/1) mixture. The solid lines represent a fit according to the spin pair interaction model ($\sigma_{\text{lipid-chol}} = -0.125\ s^{-1}$) as described in the text. (▼) Cholesterol C_{18} methyl resonance; (▲) 18:0 methylene resonance; (■) cross-peak between both signals.

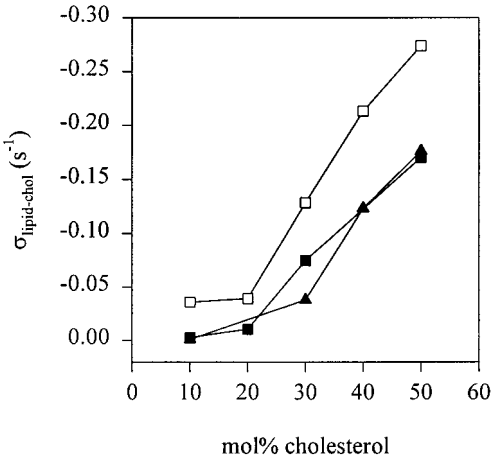

FIGURE 9: Cross-relaxation rates between the 18:0-22:6 PC chain resonances and cholesterol as a function of cholesterol concentration. Protons of the saturated chain (open symbols) have higher rates of magnetization transfer to cholesterol than protons of the polyunsaturated chain (filled symbols). (■, □) Methylene groups; (▲) vinyl groups.

cross-relaxation rates which, nevertheless, reflects the relative differences in cross-relaxation rates rather well. Protons of both saturated and polyunsaturated chains exchange magnetization with cholesterol protons as demonstrated by the existence of cross-peaks between cholesterol and both chains. The rate of cross-relaxation between the saturated chain and cholesterol (open symbols) is higher than between the polyunsaturated chain and cholesterol (filled symbols). For an ideal mixture, a linear dependence of cross-relaxation rates on cholesterol content is expected. The apparent deviation from linearity at low cholesterol content may indicate structural rearrangements in the mixture. However, even at low cholesterol concentration, magnetization transfer from saturated chains to cholesterol is higher than from polyunsaturated chains.

DISCUSSION

Chain Order Parameters. Lipid chain order parameters are a very sensitive measure of average lipid chain length

and area per molecule (*62*). Differences in chain order parameters of pure PC, PE, and PS membranes with identical hydrocarbon chains reflect differences in lipid−lipid interaction at the lipid water interface. PE molecules have, on average, more extended hydrocarbon chains and smaller area per molecules which is reflected in higher chain order parameters (*42*). PS has an intermediate, and PC the lowest lateral packing density. When PC, PE, and PS are mixed, the order parameters of *sn*-1 hydrocarbon chains of all three lipids are generally similar, indicating that the lipids mix more or less homogeneously. The small order differences between lipid species, with slightly higher order for PS, may indicate some preference for nonrandomness in lipid−lipid contacts, or a weak influence from the headgroup on chain order within the same lipid molecule.

Cholesterol is known to increase saturated chain order parameters and to reduce lipid area per molecule (*43*, *44*). This effect has been explained by the attractive van der Waals interaction between lipid chains and the steroid ring system of cholesterol (*63*). Mixed-chain polyunsaturated 18:0-22:6 phospholipids showed considerably less chain order increase than the monounsaturated 18:0-18:1 analogues, while the 22:6-22:6 PC, with two polyunsaturated chains, phase-separated from cholesterol without any chain order increase. Obviously, the van der Waals interactions between polyunsaturated chains and cholesterol are weaker, and a molecular arrangement where cholesterol has direct contact with the DHA chain is energetically less favorable. Hydrocarbon chains with cis-unsaturated double bonds may have a steric nonconformabilty with the rigid fused-ring structure of cholesterol, and, consequently, may have weaker van der Waals interactions with cholesterol than saturated hydrocarbon chains (*64*).

Qualitative information on *sn*-2 chain order was obtained from analysis of ^{1}H MAS NMR rotational sideband intensity which depends on the strength of ^{1}H−^{1}H dipolar interactions within the chains (*59*). Chains with high ^{2}H NMR order parameters also have strong ^{1}H−^{1}H dipole−dipole interactions and, consequently, strong rotational sidebands. A theoretical calculation (K. Gawrisch, unpublished result) indicates that sideband intensity at low spinning speeds (2−3 kHz) has similar sensitivity to changes in chain order as the ^{2}H NMR order parameters. However, because of signal superposition in the ^{1}H NMR spectrum of lipids, the order parameters cannot be assigned to specific chain protons. We used the sideband analysis to observe qualitative order changes of the polyunsaturated DHA chain in the presence of cholesterol. Compared to saturated chains, the DHA chain has rather low order parameters. Addition of cholesterol to mixed-chain phospholipids increased the order of the DHA chain. The method does not discriminate between an order increase as a result of direct cholesterol−DHA contacts or indirect ordering of the DHA chain via an ordering of the entire lipid matrix.

The differences in *sn*-1 chain order increase between lipids after addition of cholesterol are a reflection of preferential contacts between cholesterol and PC in the polyunsaturated mixture and, somewhat less distinct, cholesterol and PE in the monounsaturated mixture. The order of PS is influenced the least in both polyunsaturated and monounsaturated lipid mixtures, indicating a lower probability of PS−cholesterol interaction. This is in agreement with a very recent study (*24*) which predicted that cholesterol prefers interaction with PC over PS.

NOESY Cross-Relaxation Rates. The most direct measure of lipid−lipid interaction comes from the analysis of NOESY cross-relaxation rates. Cross-relaxation between resonances of different lipid species requires that their protons have approached within 5 Å (*53*). Rates depend on (i) the probability of contact between two lipid molecules, (ii) the distance between interacting protons (<5 Å), and (iii) the correlation time of motions of the distance vector. Information on lateral lipid organization is contained in the probability of contact (i) between the lipids. We minimized the potentially perturbing influence from (ii) and (iii) by investigating NOESY cross-peaks between identical molecular groups on samples with identical lipid composition. Interaction between two lipid species, e.g., PC and cholesterol, was selected by suppressing chain proton resonances of the other lipids with deuterium labeling. Two results of cross-peak analysis are most striking: (i) the cross-relaxation rates reflect the preferred interaction between PC and cholesterol in the polyunsaturated mixture first detected in the ^{2}H order parameter measurements, and (ii) rates between protons of the saturated chain and cholesterol are higher than between the polyunsaturated chain and cholesterol. This suggests a preferential association between saturated hydrocarbon chains and cholesterol which was expected after observing the total separation of 22:6-22:6 PC, containing two DHA chains, and cholesterol in 22:6-22:6 PC/cholesterol mixtures.

Docosahexaenoyl Chains and Cholesterol Trigger Lateral Phase Segregation. The larger cholesterol-induced 18:0-22:6 PC order increase in the polyunsaturated 18:0-22:6 PC/18:0-22:6 PE/18:0-22:6 PS/cholesterol mixture reflects a preferential association of 18:0-22:6 PC with cholesterol. The higher NOESY cross-relaxation rates between the cholesterol C_{18} methyl group and the *sn*-1 stearic acid chain in PC, compared to the same chain in PE and PS, confirm this conclusion. However, the NOESY experiment provides no information about the size of demixed regions, because it has a time scale equivalent to the relatively lengthy spin−lattice relaxation time of the lipid's protons (0.25 s). Within 0.25 s, at a lipid lateral diffusion rate of $D = 10^{-8}$ cm^2 s^{-1} (*65*), every lipid molecule visits a circular area with a radius of 1 μm. This is only 1 order of magnitude less than the dimensions of typical cell plasma membranes. Therefore, the NOESY cross-relaxation rates represent information averaged over almost the entire membrane.

In contrast, the ^{2}H NMR experiment has a much shorter time scale and resolves the lipid composition of significantly smaller domains or clusters. According to Table 2, the difference in quadrupole splittings between the 18:0-22:6 PC−cholesterol-enriched regions and the remaining membrane area is of the order of 1 kHz. Because the experiments generated only one set of quadrupole splittings for every lipid, the lifetime, τ, of lipid molecules in the clusters must be less than $\tau = (2\pi\Delta\nu)^{-1} = 1.6 \times 10^{-4}$ s, and the cluster radius, r, must be equal to or smaller than $r = 2(D\tau)^{1/2} =$ 250 Å. Therefore, the ^{2}H NMR experiments suggest that the demixed regions are relatively small in size. Analogous to previous publications (*4*, *66*), we call these 18:0-22:6 PC−cholesterol clusters "liquid-crystalline microdomains". The increased chain order of 18:0-22:6 PC inside the micro-

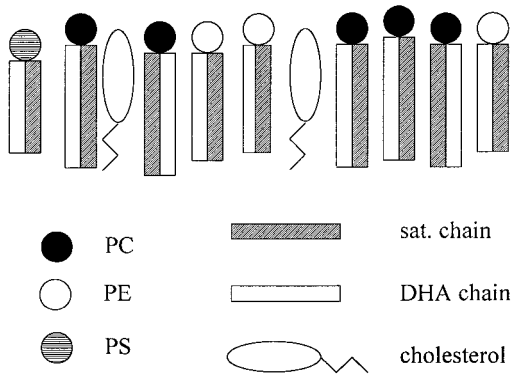

FIGURE 10: Cholesterol interacts preferentially (but not exclusively) with the saturated chain of the mixed-chain 18:0-22:6 PC in 18:0-22:6 PC/PE/PS/cholesterol mixtures. This preferential interaction results in higher *sn*-1 chain order parameters in PC compared to PE and PS. Higher chain order corresponds to, on average, somewhat longer chains. Most likely, the results reflect the formation of short-lived PC−cholesterol clusters.

domains corresponds to a 0.25 Å increase in average chain length over the surrounding lipids (*57*).

Furthermore, the NOESY results allow speculation concerning lipid organization inside the microdomains. On average, cross-relaxation rates from saturated stearic acid chains to cholesterol are higher than rates from the polyunsaturated docosahexaenoic chains to cholesterol, suggesting that the cholesterol molecules are preferentially surrounded by the saturated hydrocarbon chains of the mixed-chain PC (see Figure 10). Despite this preference, both saturated and polyunsatured chains have contact with cholesterol, and gain in molecular order from interaction with cholesterol. Therefore, a very rapid lateral rearrangement of the lipids in the membrane, that allows all contacts to occur over a brief period of time, must be assumed.

CONCLUSIONS

Chain order parameters of individual lipids in the mixture and high-resolution magic angle spinning NOESY cross-peaks between proton resonances of different lipid species offer a sensitive and local probe to study lateral lipid organization. An important feature of both NMR approaches is that they require only isotopic labeling which is unlikely to perturb lipid organization. In contrast, introduction of spin- and fluorescence-labeled lipids into the lipid matrix may perturb lipid packing. It is also notable that, in this study, judgment concerning lipid organization was solely based on data obtained in the liquid-crystalline phase, not from the possibly anomalous behavior of lipid mixtures near liquid-crystalline−gel phase boundaries.

The experiments have demonstrated that lipid chain order parameters and NOESY cross-relaxation rates between lipids reflect cholesterol-induced changes in lateral lipid organization. In the future, the same techniques may be used to investigate the influence of membrane proteins on lipid microdomain formation.

ACKNOWLEDGMENT

We thank Laura L. Holte, Burton J. Litman, and Norman Salem, Jr., for useful comments.

REFERENCES

1. Lee, A. G. (1977) *Biochim. Biophys. Acta 472*, 285−344.
2. Schram, V., Lin, H. N., and Thompson, T. E. (1996) *Biophys. J. 71*, 1811−1822.
3. Klausner, R. D., and Kleinfeld, A. M. (1984) in *Cell surface dynamics: concepts and models* (Perelson, A. S., DeLisi, C., and Wiegel, F. W., Eds.) pp 23−58, Marcel Dekker, Inc., New York.
4. Edidin, M. (1997) *Curr. Opin. Struct. Biol. 7*, 528−532.
5. Salem, N., Jr., and Niebylski, C. D. (1995) *Mol. Membr. Biol. 12*, 131−134.
6. Salem, N., Jr., and Ward, G. R. (1993) *World Rev. Nutr. Diet. 72*, 128−147.
7. Fliesler, S. J., and Anderson, R. E. (1983) *Prog. Lipid Res. 22*, 79−131.
8. Leaf, A., Gosbell, A., McKenzie, L., Sinclair, A., and Favilla, I. (1996) *Early Hum. Dev. 45*, 35−53.
9. Litman, B. J., and Mitchell, D. C. (1996) *Lipids 31*, S-193−S-197.
10. Mitchell, D. C., Straume, M., and Litman, B. J. (1992) *Biochemistry 31*, 662−670.
11. Dratz, E. A., and Holte, L. L. (1992) in *Essential fatty acids and eicosanoids: invited papers from the third International Congress* (Sinclair, A. F., and Gibson, R. A., Eds.) pp 122−127, American Oil Chemists Society, Champaign, IL.
12. Gibson, N. J., and Brown, M. F. (1993) *Biochemistry 32*, 2438−2454.
13. Boesze-Battaglia, K., Hennessey, T., and Albert, A. D. (1989) *J. Biol. Chem. 264*, 8151−8155.
14. Boesze-Battaglia, K., Fliesler, S. J., and Albert, A. D. (1990) *J. Biol. Chem. 265*, 18867−18870.
15. Ipsen, J. H., Karlstrom, G., Mouritsen, O. G., Wennerstrom, H., and Zuckermann, M. J. (1987) *Biochim. Biophys. Acta 905*, 162−172.
16. Ipsen, J. H., Mouritsen, O. G., and Zuckermann, M. J. (1989) *Biophys. J. 56*, 661−667.
17. Vist, M. R., and Davis, J. H. (1990) *Biochemistry 29*, 451−464.
18. Sankaram, M. B., and Thompson, T. E. (1991) *Proc. Natl. Acad. Sci. U.S.A. 88*, 8686−8690.
19. van Dijck, P. W., de Kruijff, B., van Deenen, L. L., de Gier, J., and Demel, R. A. (1976) *Biochim. Biophys. Acta 455*, 576−587.
20. Yeagle, P. L., and Young, J. E. (1986) *J. Biol. Chem. 261*, 8175−8181.
21. Blume, A. (1980) *Biochemistry 19*, 4908−4913.
22. Tilcock, C. P. S., Bally, M. B., Farren, S. B., and Cullis, P. R. (1892) *Biochemistry 21*, 4596−4601.
23. van Dijck, P. W. (1979) *Biochim. Biophys. Acta 555*, 89−101.
24. Bach, D., Borochov, N., and Wachtel, E. (1998) *Chem. Phys. Lipids 92*, 71−77.
25. McMullen, T. P. W., and McElhaney, R. N. (1997) *Biochemistry 36*, 4979−4986.
26. Silvius, J. R., del Giudice, D., and Lafleur, M. (1996) *Biochemistry 35*, 15198−15208.
27. Shin, Y. K., Moscicki, J. K., and Freed, J. H. (1990) *Biophys. J. 57*, 445−459.
28. Subczynski, W. K., Antholine, W. E., Hyde, J. S., and Kusumi, A. (1990) *Biochemistry 29*, 7936−7945.
29. Nakagawa, Y., Utsumi, H., Inoue, K., and Nojima, S. (1979) *J. Biochem. (Tokyo) 86*, 783−787.
30. Rujanavech, C., and Silbert, D. F. (1986) *J. Biol. Chem. 261*, 7215−7219.
31. Smaby, J. M., Momsen, M. M., Brockman, H. L., and Brown, R. E. (1997) *Biophys. J. 73*, 1492−1505.
32. Zerouga, M., Jenski, L. J., and Stillwell, W. (1995) *Biochim. Biophys. Acta 1236*, 266−272.
33. Kariel, N., Davidson, E., and Keough, K. M. W. (1991) *Biochim. Biophys. Acta 1062*, 70−76.
34. Demel, R. A., Geurts van Kessel, W. S. M., and van Deenan, L. L. M. (1972) *Biochim. Biophys. Acta 266*, 26−40.
35. Keough, K. M. W., Giffin, B., and Matthews, P. L. J. (1989) *Biochim. Biophys. Acta 983*, 51−55.
36. Morrow, M. R., Davis, P. J., Jackman, S., and Keough, K. M. W. (1996) *Biophys. J. 71*, 3207−3214.

37. Hernandez-Borrell, J., and Keough, K. M. W. (1993) *Biochim. Biophys. Acta 1153*, 277−282.
38. Stillwell, W., Dumaual, A. C., and Jenski, L. J. (1996) *Biophys. J. 70*, A90.
39. Marsh, D., Watts, A., and Smith, I. C. (1983) *Biochemistry 22*, 3023−3026.
40. Thurmond, R. L., Dodd, S. W., and Brown, M. F. (1991) *Biophys. J. 59*, 108−113.
41. Lafleur, M., Cullis, P. R., Fine, B., and Bloom, M. (1990) *Biochemistry 29*, 8325−8333.
42. Separovic, F., and Gawrisch, K. (1996) *Biophys. J. 71*, 274−282.
43. Oldfield, E., Meadows, M., Rice, D., and Jacobs, R. (1978) *Biochemistry 17*, 2727−2740.
44. Ipsen, J. H., Mouritsen, O. G., and Bloom, M. (1990) *Biophys. J. 57*, 405−412.
45. Yeagle, P. L., Hutton, W. C., Huang, C. H., and Martin, R. B. (1975) *Proc. Natl. Acad. Sci. U.S.A. 72*, 3477−3481.
46. Yeagle, P. L., Hutton, W. C., Huang, C. H., and Martin, R. B. (1976) *Biochemistry 15*, 2121−2124.
47. Forbes, J., Husted, C., and Oldfield, E. (1988) *J. Am. Chem. Soc. 110*, 1059−1065.
48. Forbes, J., Bowers, J., Shan, X., Moran, L., Oldfield, E., and Moscarello, M. A. (1988) *J. Chem. Soc., Faraday Trans. 1 84*, 3821−3849.
49. Davis, J. H., Jeffrey, K. R., Bloom, M., Valic, M. I., and Higgs, T. P. (1976) *Chem. Phys. Lett. 42*, 390−394.
50. Sternin, E., Bloom, M., and MacKay, L. (1983) *J. Magn. Reson. 55*, 274−282.
51. McCabe, M. A., and Wassall, S. R. (1995) *J. Magn. Reson. B 106*, 80−82.
52. Lafleur, M., Fine, B., Sternin, E., Cullis, P. R., and Bloom, M. (1989) *Biophys. J. 56*, 1037−1041.
53. Jeener, J., Meier, B. H., Bachmann, P., and Ernst, R. R. (1979) *J. Chem. Phys. 71*, 4546−4553.
54. Wagner, G., and Wüthrich, K. (1982) *J. Mol. Biol. 155*, 347−366.
55. Macura, S., and Ernst, R. R. (1980) *Mol. Phys. 41*, 95−117.
56. Ernst, R. R., Bodenhausen, G., and Wokaun, A. (1987) *Principles of Nuclear Magnetic Resonance in One and Two Dimensions*, Clarendon Press, Oxford.
57. Holte, L. L., Peter, S. A., Sinnwell, T. M., and Gawrisch, K. (1995) *Biophys. J. 68*, 2396−2403.
58. Gross, J. D., Costa, P. R., Dubacq, J.-P., Warschawski, D. E., Lirsac, P.-N., Devaux, P. F., and Griffin, R. G. (1995) *J. Magn. Reson. B 106*, 187−190.
59. Griffin, R. G. (1981) *Methodol. Enzymol. 72*, 108−174.
60. Herzfeld, J., and Berger, A. E. (1980) *J. Chem. Phys. 73*, 6021−6030.
61. Munowitz, M. G., and Griffin, R. G. (1982) *J. Chem. Phys. 76*, 2848−2858.
62. Koenig, B. W., Strey, H. H., and Gawrisch, K. (1997) *Biophys. J. 73*, 1954−1966.
63. Davies, M. A., Schuster, H. F., Brauner, J. W., and Mendelsohn, R. (1990) *Biochemistry 29*, 4368−4373.
64. Pasenkiewicz-Gierula, M., Subczynsky, W. K., and Kusumi, A. (1990) *Biochemistry 29*, 4059−4069.
65. Wu, E. S., Jacobson, K., and Papahadjopoulos, D. (1977) *Biochemistry 16*, 3836−3841.
66. Litman, B. J., Lewis, E. N., and Levin, I. W. (1991) *Biochemistry 30*, 313−319.

BI980078G